

Highly Constrained Back Projection (HYPR): Theory and Potential MRI Applications

O. Wieben¹, J. Velikina², W. F. Block³, J. Perry², Y. Wu², K. M. Johnson², Y. Wu⁴, F. K. Korosec¹, C. A. Mistretta¹

¹Depts. of Medical Physics and Radiology, University of Wisconsin, Madison, WI, United States, ²Dept. of Medical Physics, University of Wisconsin, Madison, WI, United States, ³Depts. of Medical Physics and Biomedical Engineering, University of Wisconsin, Madison, WI, United States, ⁴Dept. of Electrical and Computer Engineering, University of Wisconsin, Madison, WI, United States

Introduction: It is desirable for many MR applications to achieve high spatial and temporal resolution. However, k-space sampling that obeys the Nyquist theorem usually precludes simultaneous achievement of both aims. Several methods have been proposed to rapidly acquire dynamic data by exploring correlated information in k-space, in time, or in both, including UNFOLD [1], k-t BLAST [2], and reconstruction of limited-view projections [3]. Here we investigate a novel, non-iterative, unfiltered backprojection algorithm that incorporates the idea of a composite image generated from multiple time frames to constrain the backprojection process, effectively allowing for the reconstruction of a time series with higher temporal resolution while maintaining high SNR and a low artifact level.

Methods: The HYPR (Highly constrained backProjection) technique achieves high temporal resolution by severe angular undersampling with an interleaved 2D or 3D radial trajectory. An increase in SNR and reduction of streak artifacts is achieved by the incorporation of a composite image reconstructed from the projections in multiple or all time frames as shown in Figure 1. The composite image is used to spatially constrain the signal backprojected from each individual time frame. The HYPR processing also requires a normalization step in the image domain. Here projections of a time frame are divided by the projections at the identical angles computed from the composite image to compensate for the signal weighting from the composite image. The overall SNR and CNR are limited by a combination of the stochastic noise and the noise from streak artifacts. The stochastic component of the SNR in the HYPR image was derived as

$$SNR_{HYPR} = SNR_{composite} / [1 + N_f / N_v^2 + N_{pix} / (N_p N_v^2)]^{1/2},$$

where $SNR_{composite}$ is the SNR in the composite image, N_f is the number of time frames, N_v is the number of vascular pixels in the projection, N_{pix} is the number of pixels in the projection (e.g. 256 for 2D or 256 x 256 for 3D), and N_p is the number of projections per time frame. In most of our simulations, N_v is on the order of 10 and the SNR is dominated by $SNR_{composite}$. The technique was evaluated in simulations by synthesizing numerical phantoms for fMRI and MR spectroscopy and by generating undersampled time series from 2D images obtained from contrast-enhanced MRA (CE-MRA), breast perfusion, diffusion imaging, and CT perfusion to investigate artifacts and how well the temporal information is represented in the images. Subsequently, HYPR was applied to phantom studies with Gd injections and *in vivo* using PR TRICKS [4], a trajectory that combines radial in-plane encoding with Fourier encoding in the slice direction, for CE-MRA and cardiac perfusion. We also simulated the use of HYPR processing with VIPR, a truly 3D trajectory [5].

Results: In our simulations, relative to conventional Cartesian encoding, we were able to achieve frame rate accelerations of 4 in fMRI and 10 in breast perfusion imaging. For PR TRICKS applications we obtained overall acceleration factors of 13 in cardiac perfusion and 150 *in vivo* CE-MRA while still preserving a sufficient SNR and temporal evolution. Simulations were also performed for reductions in scan time in EPSI-like spectroscopic imaging by a factor of 17, a factor of 13 increase in different diffusion encoding directions per scan time, and a dose reduction in CT perfusion by 10. An example of a peripheral CE-MRA exam is shown in Fig. 2. A 512 x 512 PR TRICKS examination with 72 reconstructed coronal slices was acquired with 10 projections per slice per time frame and a frame time of 940 ms. The frame rate improvement of 150 over Fourier encoding stems from radial undersampling (factor 50) and TRICKS processing (factor 3). The standard reconstruction (left column) properly displays the enhancement pattern of the vessels but the images are of low quality due to the low SNR and streak artifacts. The HYPR reconstruction (right column) incorporates the composite image into the reconstruction process and dramatically reduces streak artifacts and improves SNR. With a VIPR trajectory, undersampling can be further increased in 3D radial scanning because the artifactual spreading of signal falls off according to $1/r^2$ as opposed to $1/r$ as in the two dimensional case.

Conclusion: We demonstrated the feasibility of the HYPR technique to dramatically increase the temporal resolution in dynamic MR applications, provide more diffusion weighted images in equal scan time, or reduce the dose in CT perfusion imaging. The maximum achievable gain from the HYPR technique is somewhat dependent on the application. For example, rapid contrast enhancement in complex structures such as spiculated tumors in the breast require the acquisition of more projections per time frame than, for example, a calf study with a very sparse signal distribution. HYPR is particularly well suited for applications with sparsely distributed signal as the SNR analysis showed. In the current implementation, the HYPR algorithm is limited to applications where there is no motion which would misalign the composite image and the projections from individual time frames. We are currently optimizing sequences and reconstruction algorithms tailored to the specific requirements of various applications.

References: [1] Madore B *et al.*, *MRM*, 42:813-28, 1999. [2] Tsao J *et al.*, *MRM*, 50: 1031-42, 2003. [3] Huang Y *et al.*, *MRM*, epub, Nov. 2005. [4] Vigen K *et al.*, *MRM*, 43: 170-6. 2000. [5] Barger AV *et al.*, *MRM*, 44:821-4, 2000 [6] Mistretta CA *et al.*, *MRM*, in press.

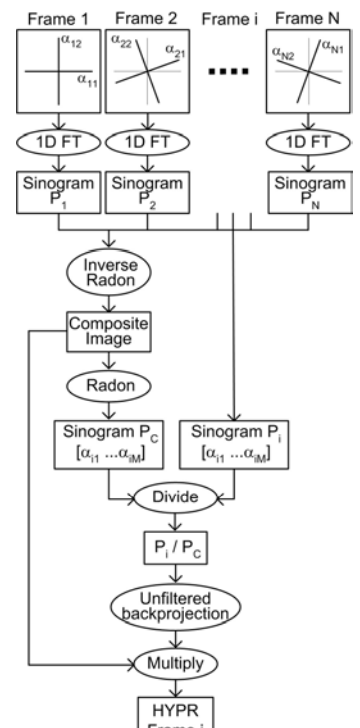


Fig 1: Block diagram of the HYPR processing.

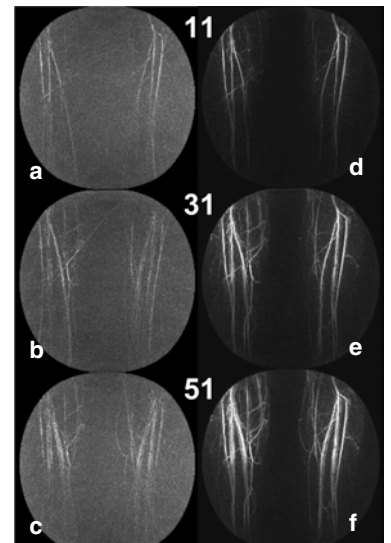


Fig. 2: Selected time frames from a peripheral 3D CE-MRA exam without (a-c) and with (d-f) HYPR processing.